Alexandria Journal of Science and Technology

Article

New mitigation approach for microbiological corrosion of carbon steel by facile separation of sodium chlorite from brine electrolysis

Shahenda Mahmoud Salem [1,*], Asaad Hassan [1], Emad Mattar [1], Howida Abouel Fetouh [2]

[1] *Chemistry Department, Faculty of Science, Damanhour University, Egypt.*

[2] *Chemistry department, Faculty of Science Alexandria university, Egypt.*

[*] *Correspondence Address:*

Shahenda Mahmoud Salem: Chemistry Department, Faculty of Science, Damanhour University, Egypt. Email address: shahendasalem0@gmail.com.

KEYWORDS: Microbiologically induced corrosion, sulfate-reducing bacteria, carbon steel, and protection.

Received:
August 11, 2024
Accepted:
November 05, 2024
Published:
November 18, 2024

ABSTRACT: The novelty of this study is the electrolysis of brine sodium chloride solution. The sustainable source is the saline seawater. A model of plug-flow electrolyzer used for continuous NaCl feed and removal of electrolysis products. Using porous cathodes graphite, pencil and new spin coated sulpher-Fe_2O_3 doped NiO composite and small anode to cathode distance achieved 98% current efficiency. The generated hypochlorous acid at the anode absorbed into sodium hydroxide solution giving efficient biocide sodium chlorite ($NaClO_2$) for mitigation of microbiologically induced corrosion (MIC) of carbon-steel. Different parameters affecting MIC have been discussed. $NaClO_2$ obtained at current density 100 $mAcm^{-2}$ passed in pure brine 1.0M NaCl solution for 30 min. using dimensional stable anode and different cathodes. Protection percentage of five wt. percentage of $NaClO_2$ against MIC reached 99% as indicated by weight loss method. The lower protection efficiency 73% and 75% from impedance and polarization respectively because these electrochemical tests are instantaneous and sufficient time provided for complete contact of biocide with SRB. Sodium chlorite is comparable biocide to formaldehyde standard biocide. The protection efficiency controlled by solubility in the aqueous SRB culture media.

1. INTRODCTION

Corrosion causes costly unscheduled shutdown time, reduced capacity and required maintenances and replacements of expensive parts. The direct and indirect losses represent 3% to 5% of the economic impact [1]. However, MIC represents fifty percentage of the corrosion costs globally. MIC initiated by acidic SRB metabolites on metal surfaces that shorten the lifetime of industrial metallic structures such as heat exchangers, cooling systems and pipelines [2]. C-steel exposed to industrial water seriously faced MIC.

Warm dirty water saturated with dissolved oxygen exposed to sunlight at temperature 30°C to 60°C, pH range 6 to 9 ensure abundant nutrients and appropriate environment for biofilm growth of SRB under anoxic conditions. Generally, MIC takes the form of pits formed underneath biofilm colonies of living organic matter such as SRB [2]. Recirculating cooling water systems ideally incubate and promoting microorganism's growth [2]. The biofilm adherent to metal surfaces alters the electrified metal/solution interface [3]. MIC caused by bacteria or fungi biofilm possessed many mechanisms and caused by microorganisms. Carbon steel constructions damaged indirectly through the corrosive chemical metabolites of SRB. The aggressive hydrogen sulphide (H_2S) formed from sulphate ions reduction by SRB. Additionally, SRB feeding on iron and consume electrons produced from the partial metal oxidation reaction, depolarizer electrons from metal surface and accelerating the oxidation rate [2, 3].

Bacteria metabolic activities producing CO_2, H_2S and organic acids wastes corrode steel pipes and causing toxicity the flowing fluids. Numerous bacteria species in hospitals environment enhanced MIC of all related steel structures in neutral stagnant water. Various bacteria such as *Bacillus*, *Pseudomonas*, *Micrococcus*, *Mycobacterium*, *Clostridium* and *Escherichia* are abundant in formation water of petroleum oils. Hydrogenase enzyme in *Escherichia* consumes molecular hydrogen, thus accelerating reduction of proton and causing MIC of steel casings and pipes. The massive biofilm

Online ISSN: 2974-3273

DOI: 10.21608/ajst.2024.311449.1046

of *Achromobacter*, *Flavobacterium* and *Desulfuricans* form polysaccharides film adherent to the porous walls causing severe plugging. MIC is recognized by the visual appearance of a black slimy nodules wastes on the pipe surface as well as underneath pitting.

The most practical efficient control method of MIC is the use of biocides to kill bacteria or inhibit growth [2]. Some biocides alter the permeability of the cell wall, thus interfering with vital life processes and reproductive cycles or damage cell by interfering with flow of nutrients and wastes discharge [4]. Biocides are either oxidizing or non-oxidizing toxicants [5]. Chlorine (Cl_2) is the common industrial oxidizing biocide. It is excellent algaecide and bactericide. The rapid hydrolysis in water yield hypochlorous acid (HOCl) and hydrochloric acid as shown in equation 1 [6-10]:

$$Cl_{2(g)} + H_2O_{(l)} \rightarrow HCl_{(aq)} + HOCl_{(aq)} \quad (1)$$

HOCl is an active species and dissociate as a function of pH, equation 2.

$$HOCl_{(aq)} \rightarrow H^+ + HOCl^-_{(aq)} \quad (2)$$

At pH 7.5 concentrations of HOCl and hypocholorous ions (OCl^-) are equals. Above pH 7.5, OCl^- species predominates. At pH 9.5, HOCl is completely ionized, therefore chorine becomes less effective in strong alkaline media. Generally, pH range 6.5 to 7.5 is practical for chlorine biocide activity. The lower pH avoided because Cl_2 accelerate corrosion. The common continuous treatment levels are 0.1 mg/L to 0.2 mg/L. The irregular treatment requires 0.5 mg/L to 1.0 mg/L dose.

Brominated compounds form hypobromous acid (HOBr) are very effective over a broad pH range than HOCl [6]. At pH 7.5, only fifty percentage HOCl and above ninety percentage HOBr present. Increasing pH to 8.7 decreases [HOCl] to 10%, but 50% HOBr remains. Non oxidizing biocides are more effective than oxidizing biocides for controlling algae, fungi and bacteria. These biocides greatly persist and are pH independent [7]. Organic-sulphur compounds include a wide variety of different biocides and the most common and efficient biocide is methylene bisthiocyanate that inhibits growth of bacteria cells by preventing transfer of energy or nutrients or the internal life-sustaining chemical reactions [8].

Electrolysis of pure NaCl gave Cl_2 gas disinfectant and the widely applicable NaOH concentrated at cathode through water evaporation. Chlorine oxidized at anode into hypochlorite and chlorite species [9]. NaOCl formed from electrolysis of dilute NaCl solutions in flow systems depending on the intensive bulk density of NaCl [10]. Conversion hypochlorite to chlorate minimized by slow agitation rate of the solution. $NaClO_2$ is a powerful oxidizing agent have various industrial and commercial applications as a bleaching agent in pulp and paper industry; bleaching and sanitizing agent in textiles; disinfectant and deodorizer for wastewater; food preservative and sanitizer. Also, $NaClO_2$ used in cleaning, etching and electroplating of the metals. It is properly stored, handled and disposed to minimize risks associated with its oxidizing properties and potential toxicity.

Ion exchange selective membrane increases the current efficiency (CE). Previous study reported electrolysis of NaCl without using selective membrane, CE of NaOCl production decreased by 3% and pH increased. Two Amperes current at flow rate 8.7 L h^{-1} of NaCl yield pure 500 ppm NaOCl solutions at 78% CE and 0.6 ppm sodium chlorate ($NaClO_3$) with 0.2% CE. On the other hand, the flow rate 9.2 L h^{-1} at 3 Ampere produced 1000 ppm NaOCl and 6 ppm $NaClO_3$ solutions respectively [10].

Nafion membrane is chemically stable selective impeded diffusion of OH^- ions to the anode, hence prevented competitive oxidation with the chlorine. The chemical structure represented in (**Figure 1**). It is a terpolymer of tetrafluoroethylene, perfluoro alkyl vinyl ether and sulfonyl acid fluoride monomers. The presence of quaternary alkyl ammonium bromide as catalyst and solvent during terpolymerization increased anion selective efficiency. The fluorocarbon backbone is hydrophobic and sulfonic acid side chain is hydrophilic.

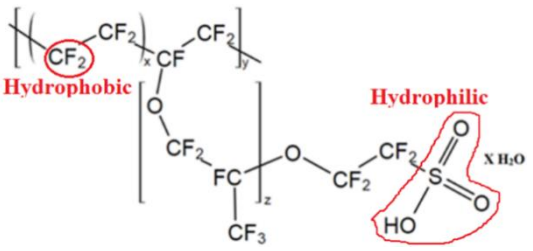

Figure 1. The main chemical structure of Nafion membrane.

The micro porosity allowed efficient exchange of sodium and chloride ions to the protons of SO_3H group and the bromide anion respectively. The mechanical strength improved durability and outstanding to mechanical stress [10]. Sustainable production of $NaClO_2$ biocides at low energy consumption was rare in the literature. The aim of the present study is scaling up production of $NaClO_2$ biocide to be used in mitigation MIC of C-steel by optimizing cathode materials using doped transition metal NiO_2@polymers composite.

2. Experimental

2.1. Materials and electrolysis method

Analytical grades chemicals: NaCl, $NiNO_3.6H_2O$ (purity 98%) (Molecular weight (Mwt. 290.794 $gmol^{-1}$) from Sigma-Aldrich, Germany, Polyethylene glycol (PEG, $C_2H_6O_2$ Mwt. 10^4 Da from Panreac, Spain, ammonium hydroxide solution 33% NH_4OH Sigma Aldrich, Na dodecyl sulphate anionic surfactant ($C_{12}H_{25}NaSO_4$ (SDS) Mwt. 288.372 $gmol^{-1}$), 99.5% NaOH pellets (R&M chemicals UK). The chemicals of culture media obtained from Sigma Aldrich Co.

The dimensionally stable anode (DSA) ruthenium oxide-titanium oxide composite (RuO_2/TiO_2 as well as graphite and pencil cathodes obtained from local commercial market of batteries.

The new NiO nanoparticles doped by sulphur and ferric oxide Fe_2O_3 prepared in 2.45 GHz-900W multimode home model microwave oven. In a closed microwave cup, (mixture $NiNO_3.6H_2O$ (14.540 g) + 2 g $Fe(NO_3)_2.H_2O$ both dissolved separately in 100 mL distilled water. 20 mL SDS solutions (5.0 g dissolved in 100 mL double distilled water + 1 wt.% PEG. pH 11 adjusted by addition of 1.0M NaOH. The microwave oven heated for 1.45 min. The precipitate washed by distilled water and filtered; dried in an electric oven for 3.0 h at

75°C. A graphite carbon rod cleaned with acetone, dried by nitrogen, spin coated by NiO nanocomposite using spin coater run at two thousand revolutions per min for 35 sec. The obtained thin film annealed at 90°C to achieve homogeneous film thicknesses. The TF coating further annealed at 450°C for 2.0h in electrical furnace and left cooling to the room temperature [11].

SRB isolated from 5.0 g soil suspended in distilled water using culture media Postgate B of chemical composition in grams: 0.5 g KH_2PO_4, 1.0 g NH_4Cl, 1.0 g Na_2SO_4, 0.1 g $CaCl_2.6H_2O$, 2.0 g $MgSO_4.7H_2O$, 5 mL of 70% Na lactate, 1.0 g yeast, 0.1g ascorbic acid, 0.1 g Thioglycollic acid, 0.5 g $FeSO_4.7H_2O$, 26 g NaCl. These constituents dissolved in 500 mL of each of seawater and double distilled water. Screw closed falcons tubes of 15 mL volume capacity autoclaved for 20 min. at 120°C and left cooled to the room temperature. 1.0 mL soil suspension water added to the tubes contain 10 mL culture media. Tubes placed in isolated jar containing anaerobic bags and 1g pyrogallol creating anoxic conditions, pH 7. After incubation for 7 days at 37°C, the black iron sulphide precipitate (FeS) formed by reaction of S^{-2} ion with Fe^{+2} ferrous ions) monitored for SRB indication bacteria growth. Serial ten folds dilution of 1.0 mL sample used for determination viable bacteria count. SRB was isolated by transfer 1mL sample from the screw capped falcons' tubes to the agar gel. SRB colonies stained by negative Gram stain and examined under stereo microscope [12].

The test solution 1.0 M NaCl used in electrolysis prepared from 4.0 M stock NaCl solution using dilution law. Simple electrolyzer, represented in (**Figure 2**) assembled. The created potential gradients along the electrodes accounted.

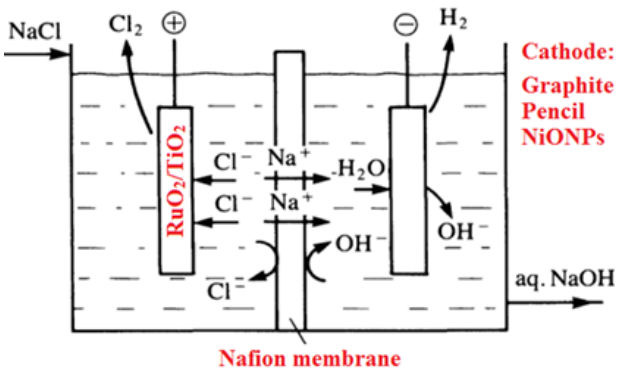

Figure 2. Schematic representation of NaCl electrolyzer using 9.0V DC power source.

The DSA RuO doped by Co_3O_4 and TiO_2 resist oxidation and corrosion by chlorine. The over potential is only 30 mV, so the oxygen evolution reaction minimized. pH of the anolyte adjusted to the range pH 6.5 to pH 7.5 using either 1.0M HCl or 1.0M NaOH. The electrolyzer of one liter volume capacity operated at stagnant conditions and the flow rate 150 $mLmin^{-1}$. The pale yellow chlorine gas liberated at anode passed through cold aqueous NaOH solution oxidized according to equation 3 into $NaClO_2$ white crystalline solid soluble in water.

$$Cl_{2(g)} + 2NaOH_{(aq)} \rightarrow NaCl_{(aq)} + NaClO_{(aq)} + H_2O \quad (3)$$

Nafion membrane used to decrease the current requirements for electrolysis by preventing migration of competitive proton and hydroxyl ions to the cathode and the anode respectively. The migration of the hydroxide ion to the anode surface neglected due to the higher transport number and smaller radius of chloride ion that increased its migration rate.

The cell potential (E_{cell}) in equation 4 expressed by negative sign due to energy consumption. The Ohmic resistance of the electrodes and the electrolyte and the external circuit accounted as IR drop respectively.

E_{cell} = (-1.2V reversible-0.5V overpotential (-1.1V-1.5V) IR drops = -4.3V (4)

$NaClO_2$ solids obtained using different cathodes differentiated by using Powder X-ray diffraction at 25°C, 2-theta angle from 5° to 75° step by 0.02°, scanning 1° $min.^{-1}$ using Bruker D8 advance diffractometer, source is copper-$K\alpha_{XR}$ of 1.5418 Å wavelength and 40 kV acceleration voltage.

2.2. Corrosion rate measurement

2.2.1. Chemical weight loss method

Corrosion coupon of carbon steel had surface area 3.38 cm^2 and the chemical composition in weight percentage (wt.%): 0.23C; 0.11Mn; 0.02Si; 0.02P; 0.02S; 0.02Ni; 0.01Cu; 0.01Cr and 99.56Fe). Corrosion rate (CR) measured chemically by weight loss method following ASTM D2688-23 standard. Each coupon was hand polished with emery papers of grades 320, 400, 600, and 1000: starting with coarse grades 320 and proceeding to the finest grade 1000 till shiny luster. The polished coupon degreased with ethanol, washed with distilled water, dried by hot air stream, weighed, then immersed in a falcon contained 100 mL SRB culture under aseptic de-aerated and sterile conditions in the tightly closed joint falcons' tubes. The dose of $NaClO_2$ was 5.0 wt. %. The test solutions incubated at 35°C for one week immersion time [10].

Each coupon taken out, surface cleaned, rinsed two times with double distilled water and degreased with ethanol and reweighed. The weight loss (Δw) determined for six weeks immersion time in the absence and the presence of 5.0 wt.% $NaClO_2$. The CR in miles per year determined using equation 5 [13]:

$$\text{Corrosion rate(mpy)} = \frac{\Delta w \times 5.34 \times 10^5}{dx\,Axt} = \frac{\Delta w \times 5.34 \times 10^5}{7.87 \times 3.38 \times t} \quad (5)$$

Where t is the immersion time (hour); *d* is the density of C-steel in (g/cm^3) and A is the surface area.

2.2.2. Electrochemical Techniques

The test solutions of the same composition as used in weight loss experiments examined by impedance and polarization measurements. Three electrodes were used: C-steel working electrode (WE) of stern-Makrides assembly design of cylindrical form inserted in white rode of polytetrafluoroethylene Teflon. Only one side of WE of surface area 1.227 cm^2 left uncovered and contact the solution. A copper wire holder attached to the metal specimen *via* screw and introduced in an insulator glass tube. Before the experiment, the surface of WE cleaned following the same polishing procedure used in weight loss measurement. Each experiment carried out using new polished electrode surface. An optical microscope was used to ensure the removal of the surface defects and coarse scratches.

Reference electrode (RE): A saturated calomel electrode (SCE) of corning type electrically contact the test solution through its

tip, so the liquid junction potential is negligible. It is a non-polarizable electrode has constant 0.242V potential at 25°C that remained constant due to the slight dependence on the temperature as shown by equation 6.

$$E_{SCE}\ (Volts) = 0.242 - 0.00078\ (t°C - 25) \quad (6)$$

Where ″t″ is the temperature in degree Celsius. The SCE periodically checked and calibrated.

Auxiliary counter electrode (AE) was an inert platinum sheet of surface area 1.0 cm^2 welded by nickel chrome wire joint insulated in glass tube. AE completed the electrical circuit and allowed current flow [13].

The electrochemical cell flat-bottom round 100 mL Pyrex flask contains three necks for insertion electrodes through tightly closed glass joints. The cell components carefully cleaned before and after each experiment to remove any foreign residues especially the metallic products. The subsequent washing using Lab. detergent solution, concentrated sulphuric acid, tap water, distilled water and a small portion of the test solution. The cell containing the test solution thermostated for 20 min. at 35°C before starting the experiment. The clean WE introduced in the cell that connected to the computerized to ACM instrument GillAC potentiostat in an experimental setup represented in (**Figure 3**).

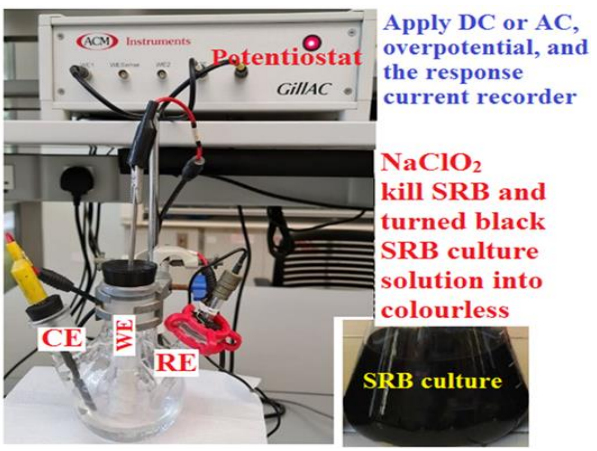

Figure 3. The experimental setup for electrochemical meaurements of CR of C-steel.

The open circuit potential (E_{OCP}) of WE followed with the immersion time until a steady state equilibrium potential attained to ensure a reliable electrochemical measurements.

The nondestructive impedance measurements carried out at the frequency range 30 k Hz to 0.1 Hz with 10 mV AC signal at E_{OCP}. The analysis of Nyquist diagrams performed by nonlinear fitting to Randles circuit using version 5 ACM analysis software program. However, in such circuit model, the double layer capacitor replaced by constant phase element (CPE) to overcome the non-ideality of capacitive behavior. The CPE depend on the frequency, reflects the interfacial heterogeneity and has an impedance function, equation 7 [13].

$$Y_{CPE}(\omega) = Y_o (i\,\omega)^n \quad (7)$$

Where the amplitude Y_o and the empirical parameter n are frequency independent and ω is the angular frequency corresponding to maximum imaginary impedance -Z''.

The exponent, n depends on the surface morphology where $-1 \le n \le 1$. The interface displaying n close to unity shows purely capacitive behavior, numerical value of capacitance of double layer (C_{dl}) approaches Y_o as n increases. In this investigation, the experimental determined values of n for the corroding steel are often around 0.99, so Randles equivalent circuit is suitable for analyzing the obtained impedance plots [14].

The double layer capacitance (C_{dl}) calculated using equation 8 [13, 14].

$$f(-Z_{max}) = 1/(2\pi\, C_{dl}\, R_{ct}) \quad (8)$$

The electrochemical theories reported the reciprocal of the charge transfer resistance ($1/R_{ct}$) is proportional to the corrosion rate.

The destructive DC potentiodynamic polarization employed by polarizing WE cathodically then anodically by starting the potential scanning from -250 mV below E_{OCP} and continuously scanning to +250 mV above E_{OCP} with scan rate 20 mV min^{-1}. Tafel plots (overpotential versus log (current density) analyzed by version5 ACM analysis software program. The polarization parameters determined by extrapolation of Tafel lines at ±50 mV around the corrosion potential [19]. These parameters include the corrosion potential ($E_{corr.}$), anodic Tafel slope (β_a), cathodic Tafel slope (β_c) and the corrosion current density (i_{corr}).

The percentage protection (%P) from the above electrochemical techniques calculated using equation 9 [13]:

$$\text{Percent protection, \%P} = \frac{Rct - Rcto}{Rct} \times 100 = \frac{io - i}{i} \times 100 \quad (9)$$

Where i_o, i, Rct_o and i, Rct are the corrosion current density and charge transfer resistance of C-steel in the presence and the absence of 5.0 wt.% sodium chlorite respectively.

3. Results and discussion

3.1. SRB and factors affecting CR

(**Figure 4**) showed isolated SRB are pure Gram negative short rods.

Figure 4. Short Gram negative rods of SRB after growth for 7 days.

SRB biofilm was colonized on surface C-steel coupons as imaged by using stereomicroscope. (**Figure 5**) showed morphology of two polished steel coupons before and after exposure to SRB culture for four days. SRB caused localized pitting corrosion as pinholes small or large in diameter [17].

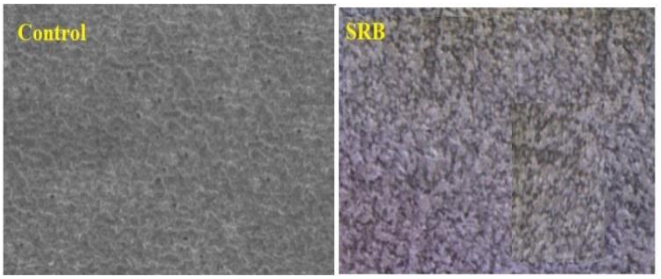

Figure 5. Surface of C-steel coupon (magnification 1.0 micron: (a) polished (b) exposed to SRB.

The reproducibility of CR determination tested using chemical weight loss method (Table 1 and **Figure 6**) carried out using three coupons immersed in SRB cultural medium at 35°C for estimating the precision of the results. The least square method applied to relate weight loss as dependent variable and immersion time as independent variable. A good straight line was obtained in each trial (correlation coefficient ($R^2 \approx 0.99$) and standard deviation range 0.0184 to 0.0190. CR were satisfactory reproducible, the series yield CR mean value 0.0575 $g.cm^{-2}.min.^{-1}$ and 0.018 standard deviation [18, 19].The parameters enhanced and retarded MIC followed the following orders respectively:

Immersion time > temperature > Na_2SO_4 > SRB inoculum and $FeSO_4$ > NaCl > $MgSO_4$.

Table 1: CR rate from 3.0 trials for mild steel exposed to SRB culture medium at 35°C.

Exposure time (week)	Trials		
	1	2	3
1	0.041	0.041	0.041
2	0.081	0.081	0.083
3	0.181	0.183	0.186
4	0.242	0.244	0.248
5	0.282	0.285	0.289
6	0.343	0.346	0.351
(CR) ($mg.cm^{-2}.min.^{-1}$)	0.057	0.057	0.058
Correlation coefficient (R^2)	0.991	0.992	0.992

CR increased by exposure time because bacteria degraded iron as a vital life component; Temperature increases the rate of MIC electrochemical MIC reaction that carries out all chemical and thermodynamic features. Na_2SO_4 strong electrolyte ionized into aggressive SO_4^{-2} to steel surface; Large SRB inoculum colony forming units isolated from soil feed on iron for sustainable life forming Fe(II) metabolite [2]. CR decreased by $FeSO_4$ because that formed partially insulated surface film protected metal surface. NaCl increasing solution conductivity retarded biofilm colonization, $MgSO_4$ act by SO_4^{-2} ion as insulating film [2].

3.2. Evaluation $NaClO_2$ on CR of MIC

Electrolysis of 0.5M NaCl solution at 25°C, flow velocity 8.0 cms^{-1}, current density 100 mA cm^{-2} continuously yield 1000 ppm $NaClO_2$ solution. The oxygen evolved at anode from water electrolysis oxidized chlorine gas into hypochlorite that slightly converted to chlorate solution, equation 1 [15, 16].

The complexity of conversion of chlorine to sodium chlorite simplified by careful control of: electrode materials. The chlorite ClO_2^- ions destroy bacteria cells by oxidizing life-sustaining cellular compounds.

3.2.1. Weight Loss Results

Table 2 showed the results of gravimetrical weight loss experiments 6 weeks immersion time during studying the effect of 5.0 wt.% $NaClO_2$ obtained from NaCl electrolysis at different cathodes. The control SRB culture and another three SRB medium.

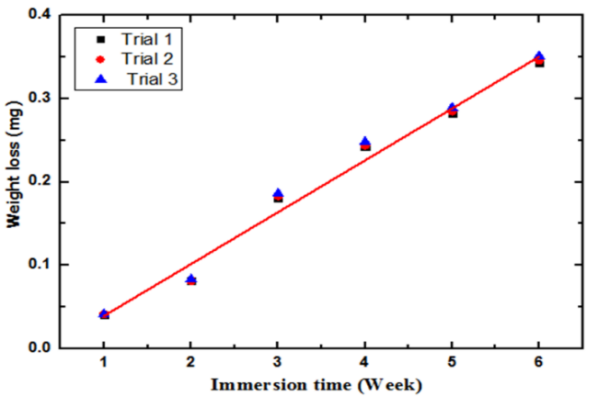

Figure 6. Test of reproducibility of CR of C-steel coupons in SRB at 35°C.

The weight decreased with increasing the exposure time for all tested solutions. The lower weight loss recorded for C-steel in SRB culture containing $NaClO_2$ [20]. (**Figures 7, 8**) showed CR of MIC calculted from the normalized weight loss data and the corresponding percentage protection (%P) respectively.

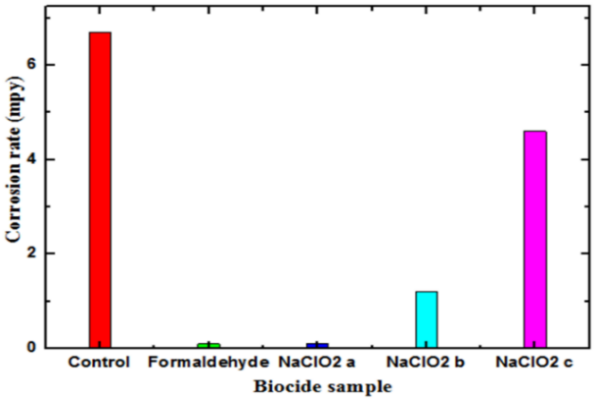

Figure 7. Variation CR rate of C-steel in SBR: $NaClO_2$ obtained at cathode: a) NiO, b) pencil and c) graphite in comparison to control and formaldehyde standard biocide.

Table 2 : Weight loss, CR of C-steel in SRB by $NaClO_4$ using different cathodes.

Exposure time (week)	Control	$NaClO_2$ obtained from different cathode materials		
		NiO nanocomposite	Pencile	Graphite
1	0.0401	0.010	0.0344	0.0734
2	0.0813		0.0344	0.0734
3	0.1815		0.0516	0.1468
4	0.2427		0.0516	0.1468
5	0.2829		0.0516	0.1835
6	0.3440		0.0688	0.2202
CR ($mg.cm^{-2}.min.^{-1}$)	0.057	ND	0.013	0.038

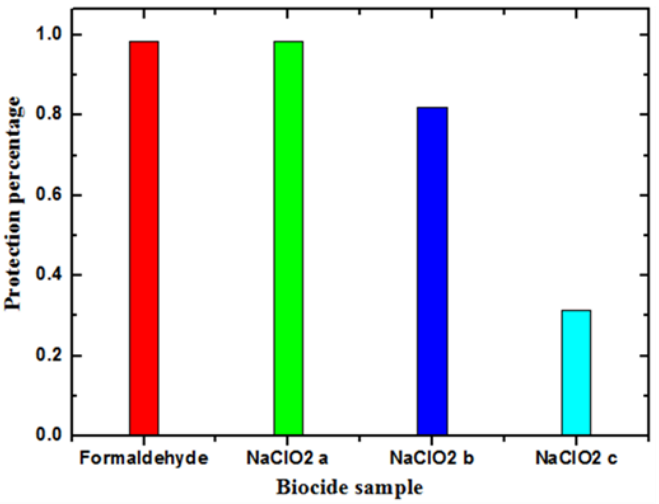

Figure 8. Variation protection percentage of $NaClO_2$ obtained at cathode: a) NiO, b) pencil and c) graphite in comparison to control and formaldehyde standard biocide.

Protection percentage of $NaClO_2$ followed the order:

$NaClO_{2a} > NaClO_{2b} > NaClO_{2c} <$ Formaldehyde (control).

At the same fixed electrolysis conditions and high current 200 $mAcm^{-2}$, NiO cathode yield pure $NaClO_2$ that dramatically decreased the rate of MIC by killing bacteria [20, 21]. Corrosion rate also affected by pH of solution, [H_2S] Hydrogen, concentration of ferrous ion and concentration of dissolved oxygen [21].

3.2.2. Electrochemical Results

3.2.2.1. Impedance Measurements

(**Figure 9**) showed Nyquist plots for C-steel in SRB in the absence and the presence of 5.0 wt.% $NaClO_2$ obtained using different cathodes.

These plots showed half semicircles indicating that steel dissolution process occurs under activation control [24]. Moreover, Nyquist plots for C-steel in SRB were characterized by a depressed semicircle of capacitive loop at high to medium frequencies region confirmed aggressiveness of SRB. Although is ClO_2^- anion adsorbed on metal surface, iron dissolution by SRB metabolites involved hydrogen reduction from the corrosive H_2S as the main metabolite product of SRB [2].

The size of the depressed semicircles (Rct) increased by the addition of 5.0wt. % $NaClO_2$ obtained using different cathodes following the order:

NiO > Pencil > Graphit > Control

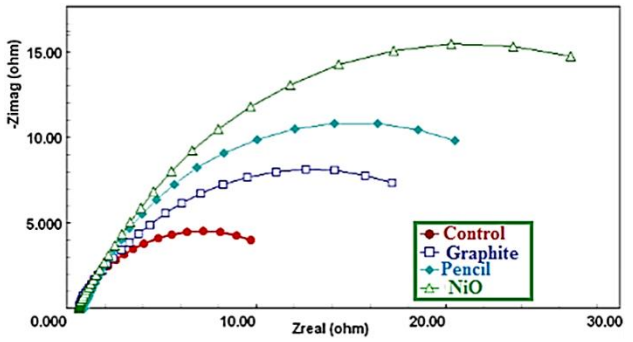

Figure 9. Nyquist plots for C-steel in SRB/$NaClO_2$ obtained using different cathodes.

Computer fitting of the Nyquist plots to the equivalent circuit analogue allowed evaluation of the solution resistance, R_s; charge transfer resistance, R_{ct} and double layer capacitance, C_{dl}. The values of these electrochemical impedance parameters are presented in Table 3.

The slight decrease in Cdl in the presence of $NaClO_2$ confirmed the main protection mechanism by killing bacteria than adsorption on the metal surface.

(**Figure 10**) showed the variations of R_{ct} and C_{dl} of steel in SRB culture in the absence and the presence of $NaClO_2$ obtained using different cathodes. The reciprocal ($1/R_{ct}$) exhibited exponential growth with rising temperature. From the electrochemical point of view, $1/R_{ct}$ is proportional to the corrosion rate in analogous to the use of polarization resistance in Stern-Geary equation 10 [18, 19].

$$i_{corr} = \left(\frac{\beta_a.\beta_c}{\beta_a+\beta_c}\right).\frac{1}{R_{ct}} = \frac{constant}{R_{ct}} \qquad (10)$$

Accordingly, at any given temperature, CR of MIC of steel significantly lowered by $NaClO_2$ produced using NiO cathode. It is an effectiveness electrocatalyst yielding more water soluble $NaClO_2$.

Table 3: The electrochemical impedance parameters of C-steel dissolution in SRB at 35°C.

Sample	R_s Ohm.cm^2	R_{ct} Ohm.cm^2	C_{dl} µF/cm^2	%P
Control	0.09	8.9	439	-
$NaClO_{2Graphite}$	0.81	20	413	0.56
$NaClO_{2Pencil}$	0.13	28	397	0.68
$NaClO_{2NiO}$	0.70	33	389	0.73

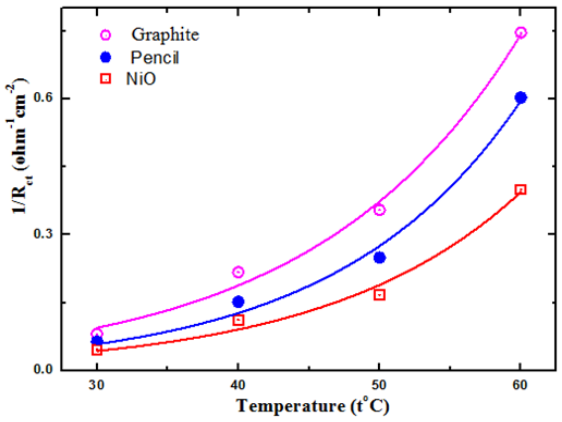

Figure 10. Variation of ($1/R_{ct}$) of C-steel dissolution in SRB temperature (°C).

3.2.2.2. Potentiodynamic polarization

The effect of $NaClO_2$ biocide obtained using different cathode materials on C-steel corrosion studied by potentiondynamic polarization. The estimated values of CR of MIC decreased by $NaClO_2$. (**Figure 11**) showed polarization curves for C-steel in SRB culture in the absence and the presence of 5.0 wt. $NaClO_2$.

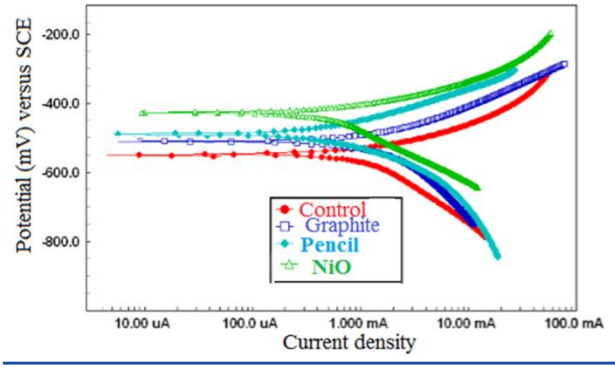

Figure 11. Polarization curves of C-steel in SRB containing different $NaClO_2$.

The polarization curves showed Tafel behavior with no diffusion current indicated that MIC is under activation control in agreement with impedance results. $NaClO_2$ shifted both the anodic and the cathodic polarization curves to higher over voltages indicated that it is mixed-type inhibitor [18, 19]. When the black FeS surface film broken down, the bare exposed areas in the film become anodic and more susceptible sites for MIC [21].

The dissolution behavior of C-steel electrode is identical in all examined SRB solutions indicating the uniform corrosion at the whole metal surface. Slight low concentration 5.0% wt. percentage $NaClO_2$ decreased CR by retarding penetration of SRB to metal surface [21]. No passivation film observed confirming that $NaClO_2$ act by biocide activity [14].

The high protection efficiency of $NaClO_2$ using NiO cathode electrocatalyst [22] because of the rapid formation of amorphous $NaClO_2$ attained on using this porous packed bed electrode. Reticular vitreous carbon support covered by S, Fe_2O_3 doped NiONPs contained interlinking pores that enhanced current flow [18, 22]. The polarization parameters for dissolution of C-steel in SRB 30 °C collected in Table 4.

The presented data clarified there is a general shift in the corrosion potential, E_{corr} towards more noble values in the presence of $NaClO_2$. The numerical values of β_a, β_c increased by NiONPs indicated retardation of steel dissolution [19].

The percentage protection of $NaClO_2$ to MIC of C-steel increased in the order:

$$i_{corr}\ (NaClO_{2graphite}) < i_{corr}\ (NaClO_{2pencil}) < i_{corr}\ (NaClO_{2NiO})$$

Inspection of (**Figure 12**) showed fairly good similarity in the recorded trend for the variation of The corrosion rate ($i_{corr.}$) of MIC increased with rising temperature in the absence and the presence of 5.0 wt.% $NaClO_2$ [23]. The $NaClO_2$ attained at NiO cathode was the most effective biocide in terms of decreasing corrosion current density [21, 23].

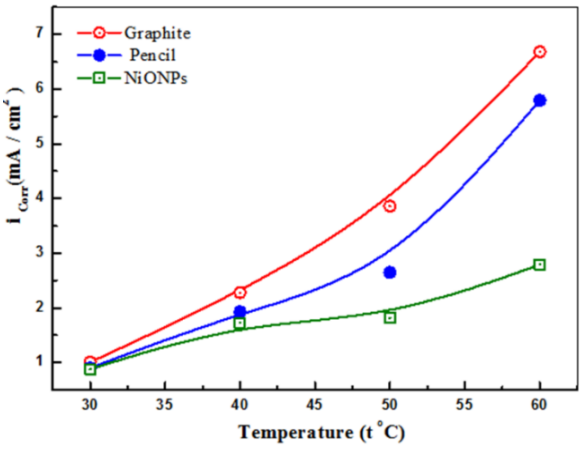

Figure 12. Variation of the corrosion rate ($i_{corr.}$) of steel in SRB with temperature.

Table 4: The electrochemical polarization parameters of steel dissolution in SRB at 35°C.

Sample	- E_{corr} (mV)	β_a (mV/decade)	- β_c (mV/decade)	$i_{corr.}$ (mA/cm^2)	%P
Control	551	83	87	3.1	
$NaClO_{2Graphite}$	489	99	90	1.5	0.52
$NaClO_{2Pencil}$	492	109	104	1.01	0.67
$NaClO_{2NiO}$	487	100	103	0.78	0.75

The lower efficiency of graphite cathode than pencil cathode attributed to the different chemical composition. Graphite is electrochemically active, only three of the four electrons in the outer valence shell of each carbon (C) atom involved in the formation of strong covalent bonds giving the layered structure. Graphite conducts electricity by the fourth delocalized electron moves free between the layers attracted to each other's by weak intermolecular forces. The more efficient pencil electrode composed mainly of graphite, small amounts of inert conducting porous clay polymer or binder resin to improve structural integrity and prevent disintegration. Trace amount of graphene oxide nanoparticles a chemical oxidized graphite added extra OH and COOH functionalization and porosity that increased the electrical conductivity in synergism with the extensive delocalized electron density.

Although the same concentration of $NaClO_2$ used in mitigation of MIC, $NaClO_2$ produced using NiO composite cathode is the most efficient. (**Figure 13**) compared powder XRD patterns of different $NaClO_2$ samples.

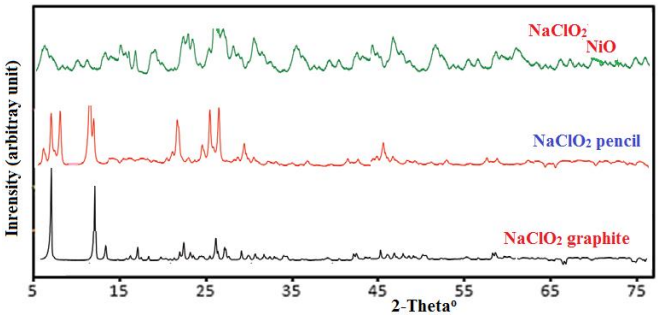

Figure 13. pXRD patterns on $NaClO_2$ obtained using different cathode materials.

The intensity of reflected XR-incidence and reflection angles plots should that $NaClO_2$ is the most amorphous sample and the hence smallest particle size. These characteristics improved solubility in aqueous SRB culture media. NiO composite cathode accelerate the rate of formation of $NiClO_2$ giving no sufficient time for crystallization.

3.3. The proposed mechanism of steel dissolution in SRB

SRB reduced SO_4^{-2} ion in the culture media into S^{-2} ions that was corrosive for steel.

Hypochlorite ion and $NaClO_2$, kill SRB and the colony forming units undetected after its addition. Sulphide ion (S^{-2}) metabolic product of SRB adsorbed on the steel surface. FeS surface complex by forms in the anodic process then desorbed from Fe surface according to equations 11, 12 [18, 19, 23]:

$$Fe + S^{-2} \rightleftharpoons (FeS)_s \text{ black insoluble corrosion product} \quad (11)$$

$$(FeS)_s \rightleftharpoons Fe^{2+} + S^{-2} \quad (12)$$

Where s represents the metal surface. Generally, if the adsorbed sulphide anion or the surface complex is stable, MIC of steel will be suppressed. Accordingly, based upon this idea, the solubility of FeS increased the corrosion rate of MIC.

The catalyst promoters S and Fe_2O_3 enhanced the performance of NiO electrocatalyst [22]. The micro porous accelerating reduction of sodium ion and Fe_2O_3 increased catalyst acidity [24].

3.4. Recommendations for the future study

NaCl electrolysis to provide low cost method for production biocides for mitigation MIC, some of challenges can be solved as represented in Table 5.

Table 5: The suggesting strategies for the common challenges in NaCl electrolysis

Challenge	Solving strategy
Costs of electricity consumption	Ion selective exchange membrane allow migration of Na^+ and Cl^- ions only and prevents migration of hydroxyl ion that passivates anode surface
Migration of proton and hydroxyl ions from water electrolysis to the oppositely charged electrodes	
Anode passivation by insulating surface impermeable oxide layer prevent current flow and decreased oxidation of Cl^-ion.	
Carbonation of cathodes	Periodical mechanical cleaning
Dissolution of conventional anode materials	Using AC current as an alternate to DC current
Ohmic losses from voltage drop by resistance of cell components and interconnections.	Minimize electrodes spacing, increasing solution conductivity by supporting electrolyte and using good electrical conductors
Concentration overvoltage	Agitation using rotating disk electrode

3.5. Sustainability of seawater as NaCl source for chlorine production

Chlorine is essential for many industrial processes and sanitation**.** The sustainability of the abundant, vast and readily available seawater as NaCl resource depends on several obstacles such as energy consumption, environmental impact and costs. Directly accessed geographic coastal regions to seawater reduced transportation costs. Energy consumed in NaCl extraction by evaporation or desalination and purification. Evaporation ponds negatively alter local ecosystems and contribute to water pollution. Desalination processes, especially reverse osmosis generate brine wastes rather than NaCl that need careful management. Various pollutants in seawater such as heavy metals, organic matter and biofilms interfere with NaCl electrolysis and must be eliminated before starting. The compliance with water quality standards confirmed by environmental regulations add costs and complications. Establishing NaCl extraction facilities and chlorine production plants near seas require significant infrastructure and economic investments. The cost of pure raw NaCl and electrodes material retard profits and commercialization.

Scaling up chlorine production into a pilot prototype plant requires overcome challenges and adopting sustainable practices for using seawater in a promising safe manner. Extraction NaCl with low electrical power; replacing expensive Nafion membrane by membranes made from natural polymers doped by ceramic silicon carbide or modified pottery ceramic clay dough; Implementing effective waste management practices such as brine recycling or legal safe environmental disposal; Research and developing new innovative technologies with low energy and no environmental impacts that must be assessed to identify and mitigate potential health risks if electrolysis products handled improperly.

$Cl_{2(gas)}$ is a reactive and toxic chemical element, irritant to skin, eyes, nose, mucous membranes and the respiratory system. Liquid chlorine causes skin ulcers. Inhalation cause coughing, chest pain, shortness of breath and pulmonary edema. Direct contact cause severe skin and eye burns. High concentrations is fatal toxic and harm aquatic life. So safety precautions requires: wear gloves, goggles and respiratory protectors when handling; storage in well-ventilated areas, developing emergency response plans and access to medical assistance in accidents. No dangers if Cl_2 handled by experienced technicians who are fully aware; trained in safety procedures follow a set of guidelines for safe storage and transportation without leakage; provided with clear safety instructions and the necessary equipment's; plans prepared to evacuate the place in the event of chlorine gas spreading and immediately adopt ascending paths, never store flammable materials near chlorine; gas cylinders not expose to direct heat, not exposed to welding in near area and securely attached to the walls using metal ties to prevent slipping.

4. Conclusion

This study involved mitigation of MIC of carbon steel by SRB colonies adherent surface biofilm. SRB culture. $NaClO_2$ confirmed as disinfectant for MIC of steel. This finding suggested scaling up chlorine and $NaClO_2$production for mitigation of MIC using simple electrolyzer. The effective variable on MIC rate are exposure time, temperature and concentration of ferrous sulphate. The dimensionally stable anode and NiO nanocomposite cathode at the appropriate distance yield $NaClO_2$ that is water solubility depending on the crystallinity. The most amorphous and fine $NaClO_2$ obtained using NiO cathode is the efficient biocide. The higher protection efficiency of $NaOCl_2$ 99% in weight loss than 73%, 75% in impedance and polarization respectively attributed to the longer contact time between $NaClO_2$ and SRB in slow weight loss method.

References

[1] Koch, G. Cost of corrosion. Trends in oil and gas corrosion research and technologies. A.M. El-Sherik ed., Production and Transmission, A volume in Woodhead Publishing Series in Energy, Elsevier; 2017. p. 3-30.

[2] Omar, S.H.; Khalil, N.E.; EL-Ahwany; A.M.D., El-Sayed, H.A.E.; Arafat, S.O.Y. Mitigation of Microbiologically Induced Corrosion (MIC) and Preventive Strategies. Research Trends of Microbiology. MedDocs eBooks http://meddocsonline.org/ Research Trends of Microbiology, MedDocs Publishers LLC; 2021. p. 1-11.

[3] Abd-El-Nabey, B.A.; Eldissouky, A.; Fetouh, H.A.; Mohamed, M.E. Role of anion in the electrochemical dissolution of copper and its inhibition by diethyl dithiocarbamate in neutral aqueous solutions. Phys. Chem. 2018, 8, 1-12.

[4] Fetouh, H.A.; Abd_Ellah, S.; Fadhil, F.M.; Ahmed, A.G.; Sallam, E.; Alazmi, M.; M Samy, A.; Taha A.; Hattawi, S.N.; El Desouky, J. Potential health risk effects of silver nanoparticles on aquatic ecosystem: Regulations and guidelines. Alexandria J. Science and Technology. 2024, 99-113.

[5] El-Shamy, A.M. A review on: biocidal activity of some chemical structures and their role in mitigation of microbial corrosion. Egyptian J. Chemistry.2020, 63, 5251-5267.

[6] Birch, R.G: a better method than “BBB” for pools with a salt-water chlorine generator. BABES for SWC pool management (V9 2023) Robert Birch. 2013, 1-26.

[7] Morris, B.E.; van der Kraan, G.M. Application of biocides and chemical treatments to both combat microorganisms and reduce (bio) corrosion. In Microbiologically influenced corrosion in the upstream oil and gas industry. CRC Press. 2017, 229-253.

[8] Sequiera, C.A.C.; Carrasquinho, P.M.N.A.; Cebola, C.M. Control of microbial corrosion in cooling water systems by the use of biocides. Microbial Corrosion.1988, 1, 240-255.

[9] Czarnetzki, L.R.; Janssen, L.J.J. Formation of hypochlorite, chlorate and oxygen during NaCl electrolysis from alkaline solutions at an RuO2/TiO2 anode, J. Applied Electrochemistry.1992. 22, 315-324.

[10] Girenko, D.V.; Velichenko, A.B.; Shmychkova, O.B. Electrolysis of NaCl solutions in flow systems. J.Chemistry and Technologies. 2021, 29, 31-41.

[11] Hasija, V.; Raizada, P.; Hosseini-Bandegharaei, A.; Singh, P.; Nguyen, V.H. Synthesis and photocatalytic activity of Ni–Fe layered double hydroxide modified sulphur doped graphitic carbon nitride (SGCN/Ni–Fe LDH) photocatalyst for 2, 4-dinitrophenol degradation. Topics in Catalysis. 2020, 63, 1030-1045.
[12] Liang, D.; Liu, X.; Woodard, T.L.; Holmes, D.E.; Smith, J.A.; Nevin, K.P.; Feng, Y.; Lovley, D.R. Extracellular electron exchange capabilities of Desulfovibrio ferrophilus and Desulfopila corrodens. Environmental Science & Technology. 2021, 55, 16195-16203.
[13] Barghout, N.A.; El Nemr, A.; Abd-El-Nabey, B.A.; Fetouh, H.A.; Ragab, S; Eddy, N.O. Use of orange peel extract as an inhibitor of stainless steel corrosion during acid washing in a multistage flash desalination plant. J. Applied Electrochemistry. 2023, 53, 379-399.
[14] Elbatouti, M.; Fetouh, H.A. Extraction of eco-friendly and biodegradable surfactant for inhibition of copper corrosion during acid pickling. Adsorption Science&Technology. 2019, 37, 649-663.
[15] Li, P.; Wang, S.; Samo, I.A.; Zhang, X.; Wang, Z.; Wang, C.; Li, Y.; Du, Y.; Zhong, Y.; Cheng, C.; Xu, W. Common-ion effect triggered highly sustained seawater electrolysis with additional NaCl production. Research.2020, 1-9.
[16] Ovando, E.; Rodríguez-Sifuentes, L.; Martínez, L.M.; Chuck-Hernández, C. Optimization of soybean protein extraction using by-products from NaCl electrolysis as an application of the industrial symbiosis concept. Applied Sciences. 2022.12, 3113-3129.
[17] Iverson, W.P. Microbial corrosion of metals. Advances in applied microbiology.1987, 32, 1-36.
[18] Hattawi, S.N.; Ahmed, A.G.; Fadhil, F.M.; Kuot, S.R.; Alsubaie, M.S.; Alazmi, M.L.; Fetouh, H.A. New approach for processing chitosan as low cost protective hybrid coating for C-steel in acid media. Heliyon.2024,10, 1-12.
[19] Fetouh, H.A. Facile route for processing natural polymers for the formulation of new low-cost hydrophobic protective hybrid coatings for carbon steel in petroleum industry. Polymer Bulletin. 2024, 1-20.
[20] Okoro, C.C. The biocidal efficacy of chlorine dioxide (ClO2) in the control of oil field reservoir souring and bio-corrosion in the oil and gas industries. Petroleum Science and Technology. 2015, 33, 170-177.
[21] Emerson, E.D. Anaerobic corrosion caused by sulfate-reducing bacteria. 1980-1989-Mines Theses & Dissertations.1987, 1-154.
[22] Fominykh, K.; Chernev, P.; Zaharieva, I.; Sicklinger, J.; Stefanic, G.; Döblinger, M.; Müller, A.; Pokharel, A.; Böcklein, S.; Scheu, C.; Bein, T. Iron-doped nickel oxide nanocrystals as highly efficient electrocatalysts for alkaline water splitting. ACS nano. 2015. 9, 5180-5188.
[23] Keshk, R.M.; Elgawad, G.E.A.; Sallam, E.R.; Alsubaie, M.S.; Fetouh, H.A. Synthesis and characterization of nicotinonitrile derivatives as efficient corrosion inhibitors for acid pickling of brass alloy in nitric acid. ChemistrySelect. 2022, 7, 1-12.
[24] Arora, A.K.; Jaswal, V.S.; Bala, R., 2018. Metal/mixed metal oxides and their applications as catalyst: a review. Asian Journal of Research in Chemistry. 2018, 11, 893-899.